A STUDY ON PHASE EQUILIBRIA IN THE CaO-Al$_2$O$_3$-SiO$_2$-"Nb$_2$O$_5$" (5 MASS PCT) SYSTEM IN REDUCING ATMOSPHERE

B. Yan[a,*], R. Guo[a], J. Zhang[a]

[a] *University of Science and Technology of Beijing, State Key Laboratory of Advanced Metallurgy, School of Metallurgical and Ecological Enginnering, Beijing, China.*

Abstract

Phase equilibria in 5 mass% "Nb$_2$O$_5$" plane of CaO-Al$_2$O$_3$-SiO$_2$-"Nb$_2$O$_5$" system at 1873K in an oxygen partial pressure of 1.78×10^{-6} Pa have been investigated through isothermal equilibration and quenching followed by EPMA examinations. In order to characterize the effect of niobium oxide on the phase relationship of the CaO-Al$_2$O$_3$-SiO$_2$ system, Nb$_2$O$_5$-containing and Nb$_2$O$_5$-free samples with the same CaO/Al$_2$O$_3$/SiO$_2$ weight ratio were investigated simultaneously. The ratios of CaO/Al$_2$O$_3$/SiO$_2$ were selected from the CaO·2Al$_2$O$_3$-liquid two-phase equilibrium region in the CaO-Al$_2$O$_3$-SiO$_2$ system at 1873 K. It was found that the adding of 5 mass% Nb$_2$O$_5$ to the CaO-Al$_2$O$_3$-SiO$_2$ system caused the original CaO·2Al$_2$O$_3$-liquid equilibrium to become three different new equilibria. The three equilibria were single liquid phase, CaO·6Al$_2$O$_3$-liquid and gehlenite-CaO·2Al$_2$O$_3$-liquid equilibrium respectively. The gehlenite phase may be a new solid solution of 2CaO·Al$_2$O$_3$·SiO$_2$ and NbO$_x$ with melting point higher than 1873 K.

Keywords: Phase equilibrium; "Nb$_2$O$_5$"- CaO-Al$_2$O$_3$-SiO$_2$ system; Reducing atmosphere.

1. Introduction

Niobium is an important alloying element in steel materials, as its addition can improve yield strength and maintain desirable toughness and ductility at the same time [1]. Niobium alloying in steel is done by adding ferroniobium into molten steel during secondary metallurgical treatment in a ladle. Therefore, the thermodynamic behavior of niobium in refining slag is important to the recovery of ferroniobium and essential to the optimization of the overall refining processes.

However, only a few investigations [2-8] have been carried out on the thermodynamic behavior of niobium in slags. Comparing with other alloying elements such as Ti and Cr etc, the affinity of niobium to oxygen is lower, so the recovery rate of niobium above 95% can be obtained. This may be the reason that thermodynamic behaviors of niobium in refining slags were not paid much attention. But it can be concluded from literatures that the thermodynamic behavior of niobium in slags are closely dependent on the slag composition and oxygen partial pressure. For example, Coley and co-works [6] found that small variations in slag composition caused the activity coefficient for Nb$_2$O$_5$ to change by over an order of magnitude in CaO-Al$_2$O$_3$-SiO$_2$-MgO system under

reducing atmosphere. Tsukihashi et al. [4] reported that adding 2% NaO$_2$ to the slag resulted in partition increases of up two orders of magnitude, in the CaO-Na$_2$O-SiO$_2$ system at 1573K using C(s)/CO(g) equilibrium to control the oxygen partial pressure. When at high oxygen potentials, Inoue et al. [7] found that the activity coefficient of Nb$_2$O$_5$ in the MgO$_{sat}$-Fe$_t$O-SiO$_2$-Nb$_x$O-MnO did not change significantly with slag composition.

In addition, the tetravalent (Nb^{4+}) and pentavalent (Nb^{5+}) valence states of niobium are present in slags [4, 8]. The factors, such as oxygen partial pressure, the slag basicity and temperature etc., influence the Nb^{5+}/ Nb^{4+} ratio in slags. For example, Mirzayousef-Jadid and co-works [8] found that the Nb^{5+}/Nb^{4+} ratio in CaO-SiO$_2$-NbO$_x$ at 1873K increased with oxygen partial pressure at a constant CaO/SiO$_2$ and constant content of total niobium. Tsukishashi et al. [4] obtained that the Nb^{5+}/Nb^{4+} ratio in CaO-SiO$_2$-CaF$_2$ slag saturated by CaO and 3CaO·SiO$_2$ at 1573K was approximately 3.

From the information mentioned above, it can be summarized that the calcium-aluminate based slags containing NbO$_x$ are important and complex system, and the investigations on the high temperature physical chemistry properties of these systems are deficient. Concerning the high temperature phase

---

equilibria of the CaO-Al$_2$O$_3$-SiO$_2$-NbO$_x$ system, there has been no report to the present author's knowledge. Therefore, in the present study, the phase equilibria of the CaO-Al$_2$O$_3$-SiO$_2$-"Nb$_2$O$_5$"(5 mass%) system at 1873 K in an oxygen partial pressure of 1.78×10^{-6} Pa were investigated, and the effect of "Nb$_2$O$_5$" on the CaO·2Al$_2$O$_3$-liquid equilibrium in the CaO-Al$_2$O$_3$-SiO$_2$ system was considered.

Experimental
2.1 Materials

The raw materials Al$_2$O$_3$, SiO$_2$ and Nb$_2$O$_5$ with purities of 99.99% were dried at 1273K for 24 hours. CaO was prepared by calcining CaCO$_3$ (Analytical grade) at 1273K for 24 hours to remove CO$_2$. These oxide powders in the desired proportions were mixed adequately in an agate mortar, and then weighed approximately 0.5 g to pressure into pellet in a steel die. The pelletized mixture was placed in a molybdenum crucible with i.d. of 9 mm, o. d of 10 mm and height of 20 mm for equilibrium experiments.

2.2 Equilibration and quenching experiments

A vertical resistance furnace with MoSi$_2$ heating elements and Al$_2$O$_3$ working tube was used. The temperature of the even temperature zone of 50 mm in length was measured using a Pt-6mass%Rh/Pt-30mass%Rh thermocouple connected to a SHIMADEN FP23 PID controller. In every experimental run, six Mo crucibles holding the samples were assembled side by side and placed at the same horizontal level in the even hot zone.

Before the furnace was heated, the reaction chamber was evacuated and filled with argon (99.999% in purity) repeatedly 3 times. As the phase relationships in the present studied system depend on oxygen potential, CO-CO$_2$ gas mixture with volume ratio of 99 to 1 was introduced into the reaction chamber with flow rate of 90 ml/min (STP) when the temperature of the furnace reached 873K, and the flow rate of argon was reduced to 60 ml /min (STP). Thereafter, the CO-CO$_2$ gas mixture and argon with volume ratio of 3 to 2 and total flow rate of 150 ml/min (STP) was passed through the furnace during the whole experiment run.

The sample first was heated to 1893 K, 20 K higher than the final equilibration temperature, for 3 hours to promote homogenization and melting of the sample, and then the temperature was lowered to 1823 K, 50 K below the equilibration temperature, for 1 hour to help crystallization of solid phases. Thereafter, the sample was held at 1873 K for 44 hours. To maintain the phase relationships at the equilibrating temperate, the samples was quenched by raising the

1. lifting device
2. gas outlet valve
3. quenching chamber
4. Mo wire
5. quenching gas inlet
6. Mo crucible
7. MoSi$_2$ rod
8. temperature controller
9. furnace tube
10. vacuum valve
11. gas inlet valve
12. B-type T.C.
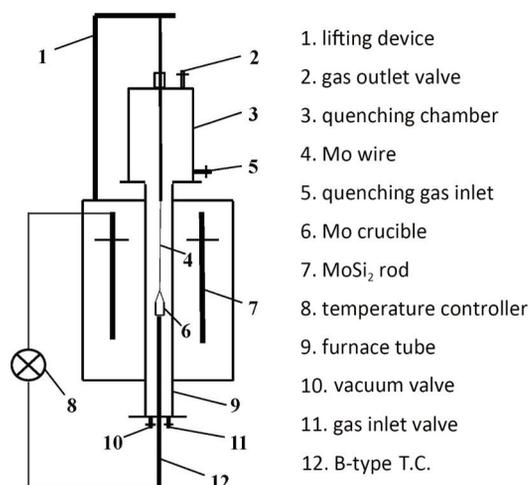
Figure 1. *Schematic diagram of the experimental apparatus*

crucibles with a speed of 30 cm/s from the even temperature zone to the water cooled quenching chamber equipped on the top of the Al$_2$O$_3$ working tube and cooling by the injected argon stream.

2.3 Phase identification

The quenched slag samples were mounted into oxy resin and polished, then carbon was deposited on the surface to get a good electric conductivity for scanning electron microscopy (SEM) and electron micro probe analyzer (EPMA) analysis. A JEOL JXA-8100 microprobe equipped with four wavelength dispersive spectrometers was employed. Six analysis points in the liquid phase and, if possible, six analysis points for each solid phase were randomly chosen. The conditions for the EPMA analysis were as follows: an accelerating potential of 15 kV, a beam current of 50 nA, and a probe diameter of 1 μm. CaSiO$_3$ was used as standard for the analysis of Ca and Si, and Al$_2$O$_3$ and Nb$_2$O$_5$ were used as standards for the analysis of Al and Nb respectively. The composition of CaO, SiO$_2$, Al$_2$O$_3$, and Nb$_2$O$_5$ were calculated using the ZAF correction method.

In some cases, X-ray diffraction was used for phase identification. The Rigaku D/MAX-RB 12KW X-ray diffractometer was adopted. Cu K$_\alpha$ was radiation used, and the 2θ scanning range was from 10 to 90º with step width of 0.02°.

3. Results

To consider the effect of "Nb$_2$O$_5$" on the phase relationship of the CaO-Al$_2$O$_3$-SiO$_2$ system, Nb$_2$O$_5$-containing and Nb$_2$O$_5$-free samples with the identical CaO/Al$_2$O$_3$/SiO$_2$ ratio were experimented simultaneously. In sample preparation, the ratios of CaO/Al$_2$O$_3$/SiO$_2$ for the samples, except 18-0 and 18-5,

were selected from the CaO·2Al$_2$O$_3$-liquid equilibrium region. The weighed-in composition data for the samples of powder mixtures are listed in Table 1.

Table 1 Weighed-in composition data for samples of powder mixtures

Sample	Weight percentage of oxide in powder mixture (%)				CaO/ Al$_2$O$_3$/ SiO$_2$
	CaO	Al$_2$O$_3$	SiO$_2$	Nb$_2$O$_5$	
5-0	32	58	10		32/58/10
	30.4	55.1	9.5	5	
6-0	30	65	5		30/65/5
	28.5	61.75	4.75	5	
7-0	30	60	10		30/60/10
	28.5	57	9.5	5	
8-0	30	58	12		30/58/12
	28.5	55.1	11.4	5	
9-0	30	55	15		30/55/15
	28.5	52.25	14.25	5	
	28.5	53.2	13.3	5	30/56/14
	30.4	53.2	11.4	5	32/56/12
17-0	27	59	14		27/59/14
	25.65	56.05	13.94	5	
18-0	45	40	15		45/40/15
	42.75	38	14.95	5	

For the quenched samples, the EPMA analyzed compositions of the liquid phase and the types of solid phases identified are listed in Table 2. Only two-phase equilibrium was found for the samples in CaO-Al$_2$O$_3$-SiO$_2$ system. As an example, figure 2 shows the backscattered electron image obtained from SEM analysis of the sample 17-0. The composition of the black phase is very close to that of CaO·2Al$_2$O$_3$ (CaO/Al$_2$O$_3$=21.54/78.46), so it should be a solid phase, while the gray phase should be a super-cooled liquid phase.
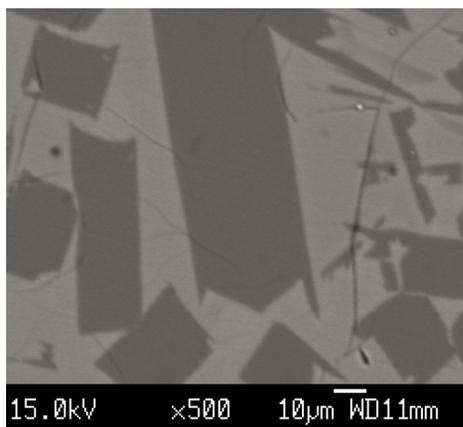
Figure 2. Backscattered electron image of sample 17-0

Three different equilibria were found in the CaO-Al$_2$O$_3$-SiO$_2$-"Nb$_2$O$_5$"(5 mass%) system. Three-phase equilibrium was found in the samples 5-5, 6-5, 7-5 and 8-5, two-phase equilibrium was observed in sample 17-5, whereas only single phase existed in the sample 9-5, 10-5 and 11-5. Figure 3 through 6 present the backscattered electron image obtained from SEM analysis of the three different equilibria in the CaO-Al$_2$O$_3$-SiO$_2$-"Nb$_2$O$_5$"(5 mass%) system. Figure 3 and 4 show the three-phase equilibrium observed in sample 5-
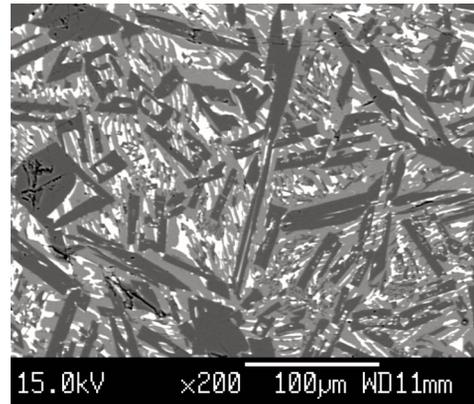
Figure 3. Backscattered electron image of sample 5-5
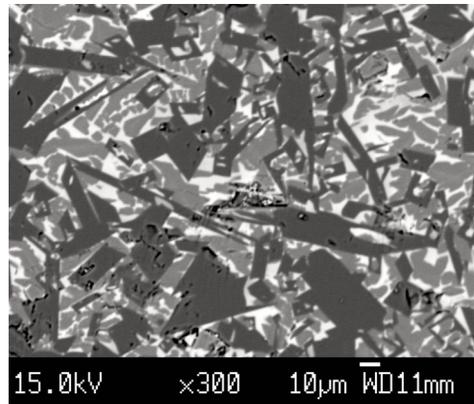
Figure 4. Backscattered electron image of sample 8-5
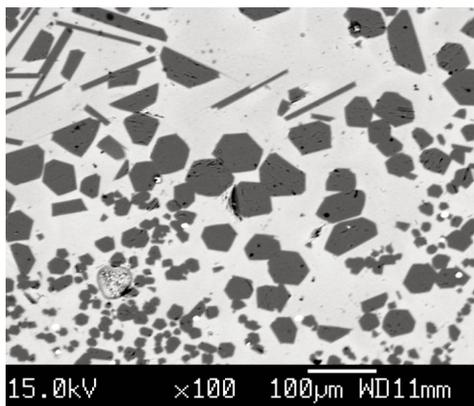
Figure 5. Backscattered electron image of sample 17-5

Table 2. *Composition of the phases measured using EPMA*

Sample	Contrast in the SEM microphotograph	Phases in equilibrium	Weight percentage in each phase from EPMA analysis			
			CaO	Al_2O_3	SiO_2	Nb_2O_5
5-0	gray	liquid	33.5	55.4	11.1	0
	black	$CaO \cdot 2Al_2O_3$	21.9	77.9	0.2	0
5-5	white	liquid	36.3	27.7	14.4	21.6
	black	$CaO \cdot 2Al_2O_3$	21.3	78.2	0.48	0.01
	gray	gehlenite	40.1	40.3	19	0.53
6-0	gray	liquid	41.1	46.3	11.6	0
	black	$CaO \cdot 2Al_2O_3$	21.5	78.5	0.05	0
6-5	white	liquid	39	27	11.1	22.9
	black	$CaO \cdot 2Al_2O_3$	21.8	78.2	0.05	0.02
	gray	gehlenite	41	40.7	17.3	1.04
7-0	gray	liquid	39.4	42.3	18.3	0
	black	$CaO \cdot 2Al_2O_3$	21.7	78.2	0.02	0
7-5	white	liquid	34.7	27.2	18.9	19.3
	black	$CaO \cdot 2Al_2O_3$	21.6	78	0.3	0.1
	gray	gehlenite	39.7	36.3	22.4	1.57
8-0	gray	liquid	38.4	40.4	21.3	0
	black	$CaO \cdot 2Al_2O_3$	21.8	77.8	0.4	0
8-5	white	liquid	25.4	29.9	19	25.8
	black	$CaO \cdot 2Al_2O_3$	20.9	79	0.08	0
	gray	gehlenite	40	37.8	21.9	0.4
9-0	gray	liquid	30.5	54.6	14.9	0
	black	$CaO \cdot 2Al_2O_3$	21.3	78.4	0.3	0
9-5	gray	liquid	27.7	53.6	13.4	5.3
10-5	gray	liquid	28.4	52.4	13.9	5.3
11-5	gray	liquid	29.6	53.1	12.3	5
17-0	gray	liquid	26.4	50.17	23.43	0
	black	$CaO \cdot 2Al_2O_3$	18.84	80.77	0.37	0
17-5	gray	liquid	24.1	52.72	17.32	5.86
	black	$CaO \cdot 6Al_2O_3$	7.13	92.55	0.22	0.11
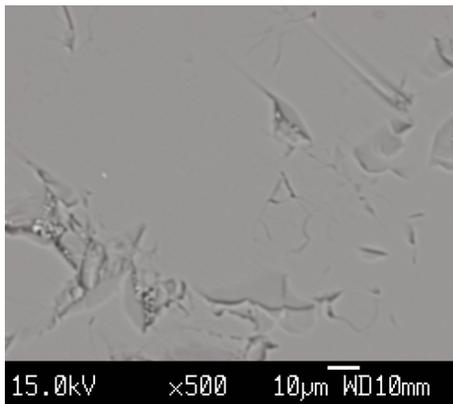
Figure 6. *Backscattered electron image of sample 10-5*

5 and 8-5 respectively. Figure 5 shows the two-phase equilibrium in sample 17-5. The single phase existed in sample 9-5, 10-5 and 11-5 is exemplified in Figure 6.

4. Discussion

For the Nb_2O_5-free samples, their weighed-in compositions were selected randomly from the $CaO \cdot 2Al_2O_3$-liquid equilibrium region of the CaO-Al_2O_3-SiO_2 system at 1873 K. As the phase relationship in the CaO-Al_2O_3-SiO_2 system does not depend on oxygen potential, the solid phase in the Nb_2O_5-free samples should be $CaO \cdot 2Al_2O_3$. From the EPMA analyzed results, it can be seen that the

composition of black phase is close to that of $CaO \cdot 2Al_2O_3$. To identify the structure of this phase, XRD analysis of sample 17-0 was carried out, and the pattern was shown in Figure 7. It can be confirmed that the solid phase is $CaO \cdot 2Al_2O_3$

Furthermore, the experimentally determined compositions for the supercooled liquid phases in equilibrium with $CaO \cdot 2Al_2O_3$ were drawn in the isothermal section of the CaO-Al_2O_3-SiO_2 system at 1873 K calculated by FactSage [9] and shown in Figure 8. It can be seen that only the compositions for the liquid phases in samples 5-0 and 9-0 agree well with that calculated by FactSage. For the other four samples, the difference between the measured and calculated composition of the supercooled liquid phase are remarkable.

Considering this difference, it should be related with the quenching rate of the samples. If the quenching rate is not fast enough, crystallization of the liquid phase will inevitable during the cooling process. This results in the composition of the supercooled liquid phase inhomogeneous, and the measured composition is not the actual composition of the liquid phase. To avoid the crystallization of the

Figure 7. XRD pattern of sample 17-0

Figure 8. Comparing of the composition measured by EPMA with phase diagram calculated by FactSage

liquid phase, the quenching rate of sample should be speeded up in future experiments, and the sample with known phase relationship and compositions should be experimented as reference.

In the present study, although the compositions of liquid phase in some samples were not measured accurately, which caused the liquidus not to be determined. But the obtained phase relationship is believable. First of all, the composition of solid phase should be unchanged during the cooling process even if the quenching rate is not fast enough. Secondly, the compositions of the solid phase in all samples were measured satisfactorily. Thirdly, the solid and liquid phases can be distinguished clearly from the microphotograph.

Concerning the three types of equilibria in the Nb_2O_5-containing samples, they are different from the liquid-$CaO \cdot 2Al_2O_3$ equilibrium existed in the Nb_2O_5-free sample in the following aspects.

First, the addition of 5 mass % Nb_2O_5 to the CaO-Al_2O_3-SiO_2 system caused the initial liquid-$CaO \cdot 2Al_2O_3$ equilibrium to alter to a single liquid phase, which can be seen clearly from the microphotograph of the samples 9-5, 10-5 and 11-5. It indicates that the addition of niobium oxide to CaO-Al_2O_3-SiO_2 system can decrease the liquidus temperature in some composition range.

Second, for the two-phase equilibrium observed in the sample 17-5, the composition of the solid phase is close to that of $CaO \cdot 6Al_2O_3$ (CaO/Al_2O_3=8.38/91.62) rather than $CaO \cdot 2Al_2O_3$. From the XRD pattern of the sample 17-5 shown in Figure 9, it can be confirmed that the solid phase is $CaO \cdot 6Al_2O_3$.

Thirdly, regarding to the three-phase equilibrium existing in the samples 5-5, 6-5, 7-5 and 8-5, the black phase shown in Figure 3 and 4 can be considered as solid $CaO \cdot 2Al_2O_3$ from the composition measured by EPMA. For the gray phase, its composition is close to $2CaO \cdot Al_2O_3 \cdot SiO_2$ ($CaO/Al_2O_3/SiO_2$=40.9/37.2/21.9) except for 1mass% Nb_2O_5, it was referred to as gehlenite in the following text. In the white phase, the
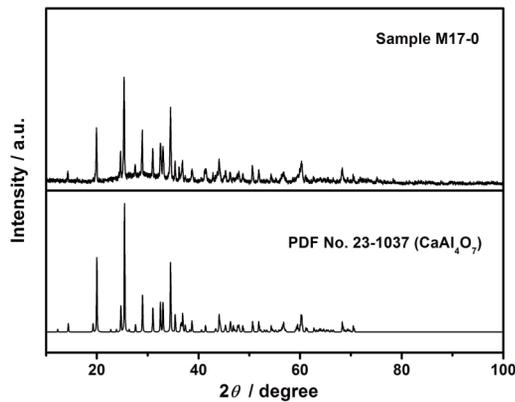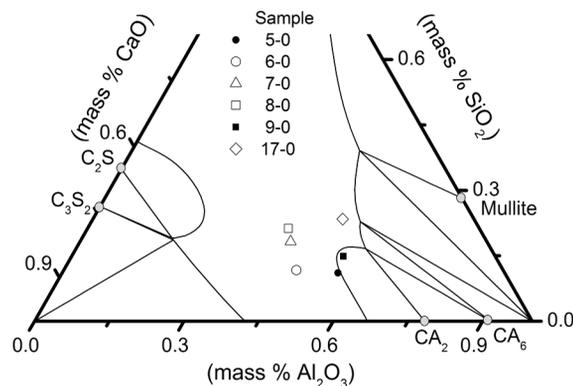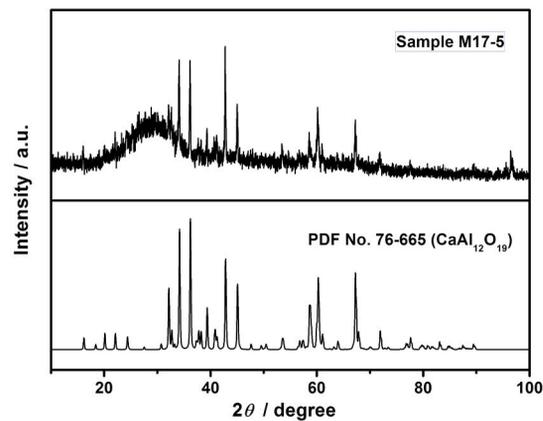
Figure 9. XRD pattern of sample 17-5

content of Nb_2O_5 measured by EPMA is as high as 20 mass %. Figure 10 presents the XRD pattern of sample 8-5 and it can be seen clearly that phases with the structure of $CaO \cdot 2Al_2O_3$ and $2CaO \cdot Al_2O_3 \cdot SiO_2$ existed.

It was reported that the melting point of $2CaO \cdot Al_2O_3 \cdot SiO_2$ is 1863K [10], 10K lower than the present experimental temperature, so the solid phase in sample 8-5 referred to as gehlenite may form during the cooling processes or is a new solid phase containing Nb with melting point higher than 1873 K. To clarify the formation of the gehlenite phase, samples 18-0 and 18-5 were investigated in the same experimental conditions as the other samples.

The weighed composition of sample 18-0 was in the primary phase field of $2CaO \cdot Al_2O_3 \cdot SiO_2$, and the sample 18-0 should be homogeneous liquid phase at 1873 K according to the phase diagram of CaO-SiO_2-Al_2O_3 system. The sample 18-5, containing mass % 5 Nb_2O_5, has the same $CaO/Al_2O_3/SiO_2$ ratio as the sample 18-0. Figures 11 and 12 show the microphotograph of the sample 18-0 and 18-5 respectively. It can be seen clearly from Figure 11 that no $2CaO \cdot Al_2O_3 \cdot SiO_2$ crystal phase can be observed in the sample 18-0, which indicated that $2CaO \cdot Al_2O_3 \cdot SiO_2$ phase could not precipitate from liquid slag under the present quenching rate.

It can be clearly seen however from the microphotograph of the sample 18-5 shown in Figure 12 that two phases existed, and the black phase should be a crystal phase. According to the EPMA results, the composition of the gray phase is also close to that of $CaO \cdot 2Al_2O_3$ (CaO/Al_2O_3=21.54/78.46) except for containing minor amount of Nb. From the XRD pattern of the sample 18-5 shown in Figure 13, it can be found that the crystal phase with a structure of $2CaO \cdot Al_2O_3 \cdot SiO_2$ existed in the sample 18-5.

Comparing the experimental results of the sample 18-5 with that of the sample 18-0, it can be seen that adding 5 mass% Nb_2O_5 caused the precipitation of a solid phase. This new solid phase has the same structure as $2CaO \cdot Al_2O_3 \cdot SiO_2$, and its composition is also close to that of $2CaO \cdot Al_2O_3 \cdot SiO_2$ except for containing minor amount of Nb. Therefore, this new solid phase may be a solid solution of $2CaO \cdot Al_2O_3 \cdot SiO_2$ and NbO_x with melting point higher than 1873 K.

Concerning the gehlenite phase in the samples 5-5, 6-5, 7-5 and 8-5, its structure is the same as that of the new solid solution in the sample 18-5, and the
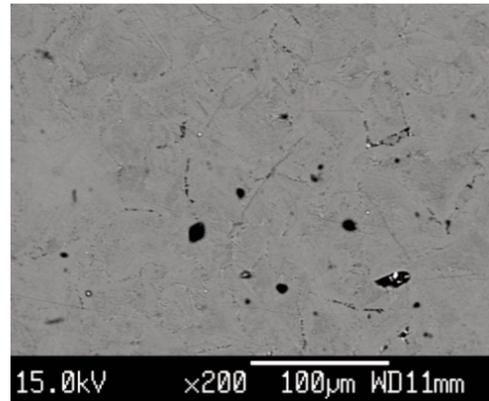
Figure 11. Backscattered electron image of sample 18-0
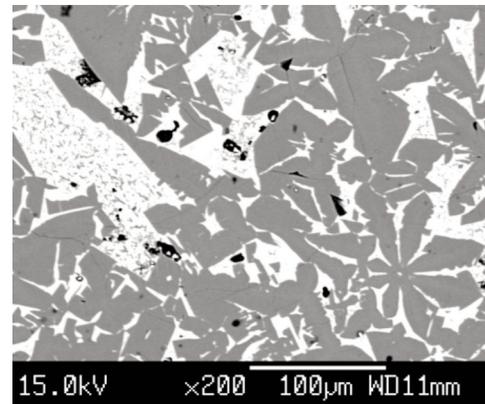
Figure 12. Backscattered electron image of sample 18-5
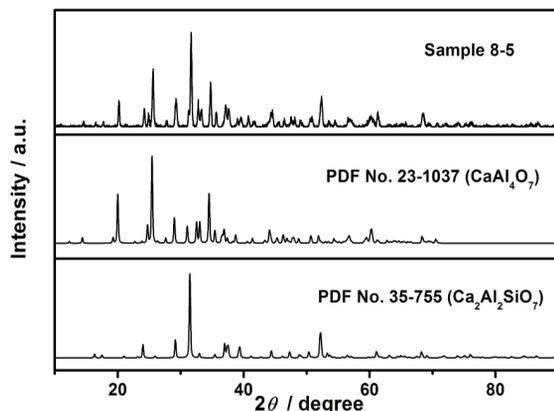
Figure 10.XRD pattern of sample 8-5
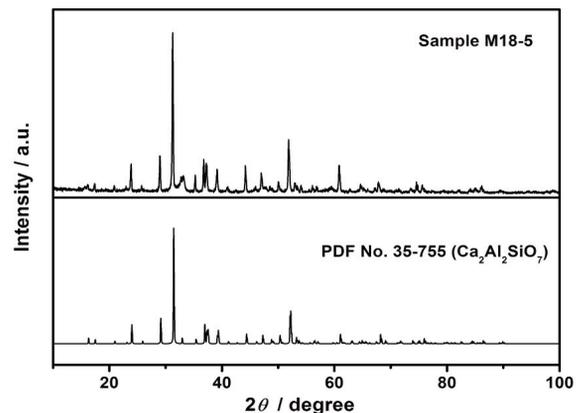
Figure 13. XRD pattern of sample 18-5

composition is very close. Therefore, it should be the same compound as the new solid solution found in the sample 18-5. That is to say, the gehlenite phase observed in the samples 5-5, 6-5, 7-5 and 8-5 is also a solid solution of $2CaO \cdot Al_2O_3 \cdot SiO_2$ and NbO_x and equilibrating with $CaO \cdot 2Al_2O_3$ and liquid at 1873 K.

5. Conclusions

The phase equilibria of some samples in the $CaO\text{-}Al_2O_3\text{-}SiO_2\text{-}$"$Nb_2O_5$" system at 1873 K were investigated in an oxygen partial pressure of 1.78×10^{-6} Pa, and the effect of "Nb_2O_5" on the $CaO \cdot 2Al_2O_3$-liquid equilibrium in the $CaO\text{-}Al_2O_3\text{-}SiO_2$ system was considered. It was found that when 5 mass% Nb_2O_5 was added to the $CaO\text{-}Al_2O_3\text{-}SiO_2$ system, the original $CaO \cdot 2Al_2O_3$-liquid equilibrium changed to three new different equilibria. The three new equilibria were single liquid, $CaO \cdot 6Al_2O_3$-liquid and gehlenite-$CaO \cdot 2Al_2O_3$-liquid equilibrium respectively. Considering the gehlenite phase, it may be a new solid solution of $2CaO \cdot Al_2O_3 \cdot SiO_2$ and NbO_x with melting point higher than 1873 K.

References

[1] S.A. Argyropoulos and P.G. Sismanis. Metall. Trans B., 22(4)B (1991) 417-427.

[2] R. Inoue and H. Suito. Transactions of the Iron and Steel Institute of Japan, 23 (7) (1983) 586-592.

[3] A. Sato, G. Aragane, A. Kasahara, et al. Tetsu to Hagane, 73 (2) (1987) 275-282.

[4] F. Tsukihashi, A. Tagaya and N. Sano. Trans. ISIJ, 28 (3) (1988) 164 - 171.

[5] S. B. Zhang, S. K. Wei, R. Y. Wang et al. Acta Metallurgica Sinica (English Edition), 3 (1) B (1990) 231-235.

[6] K.D. Bonnet and K.S. Coley. 60th Ironmaking Conf. Proceedings, Iron and Steel Society, Baltimore 2001, MD (60) 965-972.

[7] R. Inoue, X.P. Zhang, H. Li, et al. Trans. ISIJ 27 (12) (1987) 946-950.

[8] A.M. Mirazyouser-Jadid and K. Schwerdtfeger. Metall. Mater. Trans B., 41 (1) B (2011) 1038-1041.

[9] A. D. Pelton, FactSage, a computer software, Centre de Recherche en Calcul Thermochimique, Dép. de Génie Chimique, 2010.

[10] E. F. Osborn and J. F. Schairer. Am. J. Sci., 239 (1) (1941) 715-763.